ELSEVIER

Journal of Biomechanics 34 (2001) 153–161

JOURNAL OF BIOMECHANICS

www.elsevier.com/locate/jbiomech
www.JBiomech.com

1999 ASB Pre-Doctoral Award

Static and dynamic optimization solutions for gait are practically equivalent

Frank C. Anderson[a,*], Marcus G. Pandy[a,b]

[a]Department of Mechanical Engineering, The University of Texas at Austin, Austin, Texas, USA
[b]Department of Kinesiology and Health Education, The University of Texas at Austin, Austin, Texas, USA

Accepted 3 July 2000

Abstract

The proposition that dynamic optimization provides better estimates of muscle forces during gait than static optimization is examined by comparing a dynamic solution with two static solutions. A 23-degree-of-freedom musculoskeletal model actuated by 54 Hill-type musculotendon units was used to simulate one cycle of normal gait. The dynamic problem was to find the muscle excitations which minimized metabolic energy per unit distance traveled, and which produced a repeatable gait cycle. In the dynamic problem, activation dynamics was described by a first-order differential equation. The joint moments predicted by the dynamic solution were used as input to the static problems. In each static problem, the problem was to find the muscle activations which minimized the sum of muscle activations squared, and which generated the joint moments input from the dynamic solution. In the first static problem, muscles were treated as ideal force generators; in the second, they were constrained by their force–length–velocity properties; and in both, activation dynamics was neglected. In terms of predicted muscle forces and joint contact forces, the dynamic and static solutions were remarkably similar. Also, activation dynamics and the force–length–velocity properties of muscle had little influence on the static solutions. Thus, for normal gait, if one can accurately solve the inverse dynamics problem and if one seeks only to estimate muscle forces, the use of dynamic optimization rather than static optimization is currently not justified. Scenarios in which the use of dynamic optimization is justified are suggested.

Keywords: Dynamic optimization; Static optimization; Gait; Articular contact forces; Muscle forces

1. Introduction

Static optimization, an inverse dynamics approach, has been used extensively to estimate in vivo muscle forces during gait (Seireg and Arvikar, 1975; Pedotti et al., 1978; Hardt, 1978; Crowninshield et al., 1978; Crowninshield and Brand, 1981; Patriarco et al., 1981; Röhrle et al., 1984; Brand et al., 1986; Pedersen et al., 1997; Glitsch and Baumann, 1997). Static models are computationally efficient, have allowed full three-dimensional motion, and have generally incorporated 30 or more muscles per leg. However, static optimization has been criticized on several points. First, the inverse dynamics problem is highly dependent on the accurate collection and processing of body segmental kinematics (Patriarco et al., 1981; Davy and Audu, 1987). Second, while it is purportedly necessary to account for the underlying physiological properties of muscle in order to obtain more accurate estimates of muscle force (Hardt, 1978; An et al., 1989; Kaufman et al., 1991; Prilutsky et al., 1997), the time-independent nature of static optimization makes it relatively difficult to incorporate muscle physiology properly. Third, the time-independence of the performance criterion required by static optimization may not permit the objectives of the motor task to be properly characterized (Hardt, 1978; Pandy et al., 1995). Finally, analyses based on an inverse dynamics approach may not be appropriate for explaining muscle coordination principles (Kautz et al., 2000; Zajac, 1993).

Dynamic optimization, a forward dynamics approach, is not subject to these criticisms, and ostensibly can provide more realistic estimates of muscle force. Dynamic optimization integrates system dynamics into the

* Correspondence address. Biomechanical Engineering Division, Department of Mechanical Engineering, Stanford University, Stanford, California 94305-3030, USA. Fax: 650-725-1587.
E-mail address: fca@stanford.edu (F.C. Anderson).

0021-9290/01/$ - see front matter
PII: S0021-9290(00)00155-X

solution process: quantities like muscle forces and the performance criterion are treated as time-dependent state variables whose behavior is governed by sets of differential equations (Hatze, 1976). Ideally, the differential equations accurately represent the underlying physiological properties of the system, and so the time histories of muscle forces predicted are consistent with those forces which could naturally arise during movement.

Unfortunately, dynamic optimization incurs so much computational expense that relatively few dynamic solutions for gait have been found (Chow and Jacobson, 1971; Davy and Audu, 1987; Yamaguchi and Zajac, 1990; Tashman et al., 1995). Further, for gait, this approach has required that the dynamic models be simplified to such an extent that it has been difficult to ascertain whether its computational expense is justified. While Davy and Audu (1987) solved static and dynamic optimization problems for gait as part of the same study and found differences between the two solutions, it is difficult to draw conclusions based on these differences because (1) the authors simulated only the swing phase of gait, (2) the model was confined to the sagittal plane and included only nine muscles, and (3) the joint moments used as input to the static optimization problem were different from those predicted by the dynamic optimization solution.

The aim of this work is to assess whether or not dynamic optimization provides more realistic estimates of muscle force than static optimization. In particular, we address the following questions:

When estimating in vivo muscle and joint contact forces during gait

(1) Is the large computational cost of dynamic optimization justified?
(2) Is it important to account for muscle physiology, namely activation dynamics and the force–length–velocity properties of muscle?

The basis for the assessment is a comparison of a previously attained dynamic optimization solution for gait (Anderson, 1999; Anderson and Pandy, submitted) with two analogous static optimization solutions, one in which the force–length–velocity properties of muscle were taken into account and one in which they were neglected. The musculoskeletal model used allowed three-dimensional motion of the body parts and simulation of a full gait cycle. Furthermore, the model was actuated by a number of muscles which approaches that used in earlier static optimization models. Significantly, the joint torques predicted by the dynamic optimization solution were used as input to the static optimization problems. In this way, the experimental errors endemic to solving the inverse dynamics problem were eliminated, and the results of the static and dynamic optimization solutions could be compared more directly.

2. Methods

2.1. Musculoskeletal model

The body was modeled as a 10-segment, 23-degree-of-freedom linkage (Fig. 1). The inertial properties of the segments were based on anthropometric measures obtained from five healthy adult males (age 26 ± 3 yr, height 177 ± 3 cm, and mass 70.1 ± 7.8 kg) (McConville et al., 1980). Interactions of the feet with the ground were modeled using a series of spring-damper units distributed under the sole of each foot (Anderson and Pandy, 1999).

The model was controlled by a total of 54 musculotendinous actuators (Fig. 2). Each leg was controlled by 24 actuators. Relative movements of the pelvis and upper body were controlled by six abdominal and back actuators. Each actuator was modeled as a three-element, Hill-type muscle in series with tendon (Zajac, 1989). The muscle parameters, as well as the origin and insertion sites, were based on data reported by Delp (1990). The actions of ligaments were used to prevent anatomically infeasible joint angles from arising during a simulation. Each ligament was modeled as an exponential curve which provided a restoring torque about a joint axis as a function of joint angle (Davy and Audu, 1987). For

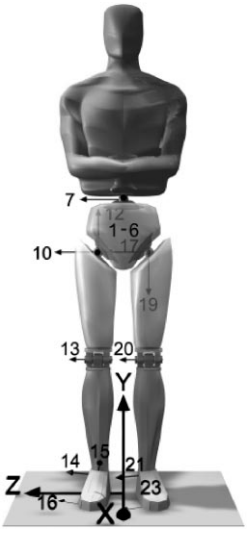

Fig. 1. Model of the body. The first six-degrees-of-freedom were used to define the position and orientation of the pelvis relative to the ground. The remaining nine segments branched out in an open chain from the pelvis. The head, arms, and torso were represented as a single rigid body which articulated with the pelvis via a three-dof ball-and-socket joint located at approximately the third lumbar vertebra. Each hip was modeled as a three-dof ball-and-socket joint, each knee as a one-dof hinge joint, each ankle-subtalar joint as a universal joint with a single joint center, and each metatarsal joint as a hinge joint. The directions of the knee, ankle, subtalar, and metatarsal joint axes were anatomical and based on in vivo and cadaveric measurements (Inman, 1976; Anderson, 1999; Anderson and Pandy, 1999).

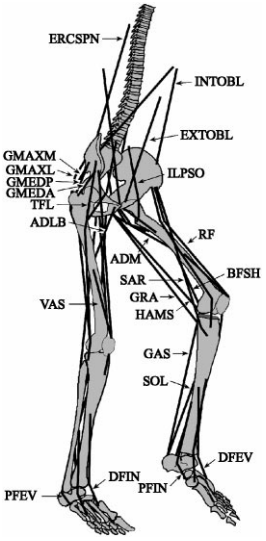

Fig. 2. Muscles in the model. Abbreviations used for the muscles are as follows: (ERCSPN) erector spinae; (EXTOBL) external abdominal obliques; (INTOBL) internal abdominal obliques; (ILPSO) iliopsoas; (ADLB) adductor longus brevis; (ADM) adductor magnus; (GMEDA) anterior gluteus medius and anterior gluteus minimus; (GMEDP) posterior gluteus medius and posterior gluteus minimus; (GMAXM) medial gluteus maximus; (GMAXL) lateral gluteus maximus; (TFL) tensor fasciae latae; (SAR) sartorius; (GRA) gracilis; (HAMS) semimembranosus, semitendinosus, and biceps femoris long head; (RF) rectus femoris; (VAS) vastus medialis, vastus intermedius, and vastus lateralis; (BFSH) biceps femoris short head; (GAS) gastrocnemius; (SOL) soleus; (PFEV) peroneus brevis and peroneus longus; (DFEV) peroneus tertius and extensor digitorum; (DFIN) tibialis anterior and extensor hallucis longus; (PFIN) tibialis posterior, flexor digitorum longus, and flexor hallucis longus. Muscles included in the model but not shown in the diagram are: (PIRI) piriformis; (PECT) pectinius; (FDH) flexor digitorum longus/brevis and flexor hallucis longus/brevis and; (EDH) extensor digitorum longus/brevis and extensor hallucis longus/brevis.

details concerning the model refer to Anderson (1999) and Anderson and Pandy (1999).

2.2. Dynamic optimization problem

A fixed-final-time dynamic optimization problem was solved for one cycle of normal gait. Because the gait cycle was assumed to be bilaterally symmetric, it was only necessary to simulate one-half of the gait cycle. The initial states were obtained by averaging kinematic and force platform data obtained from five subjects. The final time for the dynamic optimization problem was fixed to the average time taken by the five subjects to complete half of a gait cycle, which was 0.56 s.

The excitation history for each muscle was parameterized by 15 nodal points which were allowed to vary continuously between zero and one, zero indicating no excitation and one indicating maximal excitation. The nodal points representing the muscle excitations, together with the initial activation level for each muscle, served as controls in the dynamic optimization problem:

$$u_m^1, \ldots, u_m^{15}, \qquad a_m(0), \quad m = 1, \ldots, 54, \tag{1}$$

where u_m^i is the ith muscle excitation node for muscle m and $a_m(0)$ is the activation level of muscle m at $t = 0$ in the simulation. The dependence of muscle activation level on excitation level was described by a first-order differential equation

$$\dot{a} = (u^2 - ua)/\tau_{\text{rise}} + (u - a)/\tau_{\text{fall}}, \quad a = a_m(t), \quad u = u_m(t), \tag{2}$$

where $a_m(t)$ is the activation level of muscle m at time t, $u_m(t)$ is the excitation level of muscle m at time t, and τ_{rise} (22 ms) and τ_{fall} (200 ms) are the rise and decay constants of muscle activation (Pandy et al., 1992).

The dynamic optimization problem was minimally constrained: only those constraints necessary to ensure a repeatable gait cycle were imposed. Specifically, terminal boundary constraints were applied to the joint angular displacements, joint angular velocities, muscle activation levels, and muscle excitation levels so that the states at the end of the simulation were approximately equal to those at $t = 0$. Because only one-half of the gait cycle was simulated, terminal states for the left-hand side of the body were constrained to equal the initial states for the right-hand side of the body, and vice-versa:

$$q_i^{\text{cl}}(t_{\text{f}}) = q_i(0), \quad i = 4, \ldots, 23, \tag{3}$$

$$\dot{q}_i^{\text{cl}}(t_{\text{f}}) = \dot{q}_i(0), \quad i = 4, \ldots, 23, \tag{4}$$

$$a_m^{\text{cl}}(t_{\text{f}}) = a_m(0), \quad m = 1, \ldots, 54, \tag{5}$$

$$u_m^{15,\text{cl}} = u_m^1, \quad m = 1, \ldots, 54, \tag{6}$$

where $q_i(t)$ and $\dot{q}_i(t)$ are the ith generalized coordinate and generalized velocity of the model, respectively, $a_m(t)$ is the activation level of muscle m, and u_m^{15} and u_m^1 are the 15th and 1st control node for muscle m, respectively. The superscript cl indicates the contralateral quantity. For example, in Eq. (5) the contralateral quantity is the activation level of the contralateral muscle. Note that constraints were not placed on the generalized coordinates or velocities relating to the translation of the pelvis (i.e, $i = 1, \ldots, 3$ in Eqs. (3) and (4)).

There is much experimental evidence to suggest that people select walking speeds which minimize the metabolic energy expended per unit distance traveled (Ralston, 1958,1976; Corcoran and Brengelmann, 1970; Finley and Cody, 1970). The performance criterion for the dynamic optimization problem was therefore expressed as follows

$$J = \frac{\int_0^{t_{\text{f}}} \left(\dot{B} + \sum_{m=0}^{54} (\dot{A}_m + \dot{M}_m + \dot{S}_m + \dot{W}_m) \right) \mathrm{d}t}{X_{\text{cm}}(t_{\text{f}}) - X_{\text{cm}}(0)}, \tag{7}$$

where the numerator is a computation of the total metabolic energy consumed and the denominator is the change in position of the center of mass in the direction of progression. The equations used to estimate metabolic energy from the internal states of the muscles were developed based largely on the work of Davy and Audu (1987), Hatze and Buys (1977), and Mommaerts (1969). $\dot{B}$ is the basal metabolic rate of the whole body. For muscle m, $\dot{A}_m$ is the activation heat rate, $\dot{M}_m$ is the maintenance heat rate, $\dot{S}_m$ is the shortening heat rate, and $\dot{W}_m$ is the mechanical work performed (Anderson, 1999).

Hyper-extension of the joints was penalized by appending the following function to the performance criterion:

$$\phi(t_f) = w \int_0^{t_f} \left(\sum_{j=1}^{17} T_{\mathrm{lig}_j}(t)^2 \right) \mathrm{d}t, \tag{8}$$

where $T_{\mathrm{lig}_j}(t)$ is the torque applied by the ligaments about joint axis j at time t, and w (0.001) is a weight factor. The performance criterion was therefore augmented

$$J' = \frac{\int_0^{t_f} \left(\dot{B} + \sum_{m=0}^{54} (\dot{A}_m + \dot{M}_m + \dot{S}_m + \dot{W}_m) \right) \mathrm{d}t}{X_{\mathrm{cm}}(t_f) - X_{\mathrm{cm}}(0)} + \phi(t_f). \tag{9}$$

Thus, the dynamic optimization problem was to find values of the controls (Eq. (1)) such that the constraints (Eqs. (3)–(6)) were satisfied and the performance criterion (Eq. (9)) was minimized. Note that the dynamic equations for the skeleton (not shown), for the muscle forces (not shown), and for the muscle activations (Eq. (2)) were also constraints in the dynamic problem and were enforced implicitly by numerically integrating these equations forward in time during the simulation. The dynamic optimization problem was solved using a parallel parameter optimization algorithm (Pandy et al., 1992; Anderson et al., 1995).

2.3. Static optimization problems

So that the static and dynamic solutions could be compared more directly, the joint angular displacements, joint angular velocities, and muscular joint moments predicted by the dynamic optimization solution were input into the static optimization problem, as though these quantities came from experimental measures. In this way, imprecision in the collection and processing of experimental data and errors in the estimation of body anthropometry were eliminated.

Following the example of Kaufman et al. (1991), in order to account for the force–length–velocity properties of each muscle, the muscle activation levels were used as the controls in the static optimization problems:

$$a_m(t_i), \quad m = 1, \ldots, 54, \quad i = 1, \ldots, 172, \tag{10}$$

where $a_m(t_i)$ is the activation level of muscle m at a discrete time step designated by t_i. The simulation interval (i.e., $0.0 \leqslant t \leqslant 0.56$) was broken into 172 segments, and a static optimization problem was solved at each t_i. Activation dynamics was neglected.

To assess the importance of incorporating muscle physiology, one static optimization problem was solved neglecting the force–length–velocity properties of muscle, and a second was solved with these properties included. In both cases, at each discrete time step, t_i, the force output of each muscle was computed from its activation level, $a_m(t_i)$. In the "non-physiological" case, each muscle was assumed to be an ideal force generator

$$F_m(t_i) = a_m(t_i) F_m^o, \tag{11}$$

where $F_m(t_i)$ is the force generated by muscle m and F_m^o is its maximum isometric force. In the "physiological" case, the force generated by a muscle was constrained by its force–length–velocity properties:

$$F_m(t_i) = a_m(t_i) f(F_m^o, l_m, v_m), \tag{12}$$

where the function $f(F_m^o, l_m, v_m)$ is the general force–length–velocity surface for muscle assumed in the musculoskeletal model, and l_m is the length and v_m the shortening velocity of muscle m (Zajac, 1989). Muscle lengths and shortening velocities were computed from the joint angular displacements and velocities predicted by the dynamic optimization solution, with tendon compliance and muscle pennation angle taken into account.

The force outputs of the muscles were constrained to produce the muscular joint moments predicted by the dynamic optimization solution

$$\sum_{m=1}^{54} F_m(t_i) r_{m,j}(t_i) = T_j(t_i), \quad j = 7, \ldots, 23, \quad i = 1, \ldots, 172, \tag{13}$$

where $F_m(t_i)$ is the force generated by muscle m, $r_{m,j}(t_i)$ is the moment arm of muscle m about the jth joint axis, and $T_j(t_i)$ is the muscular joint moment acting about the jth joint axis as predicted by the dynamic optimization solution. Note that Eq. (13) begins with $j = 7$, the flexion–extension axis of the back. Because the first six degrees-of-freedom concerned the displacement and orientation of the pelvis relative to the ground (see Fig. 1), no muscular moments were exerted about these generalized coordinates.

The performance criterion was to minimize activation squared, summed across all muscles (Kaufman et al., 1991; Crowninshield and Brand, 1981):

$$J_i = \sum_{m=1}^{54} (a_m(t_i))^2, \quad i = 1, \ldots, 172. \tag{14}$$

In the non-physiological case (Eq. (11)), note that muscle activation is equal to muscle stress multiplied by

some proportionality constant

$$a_m = \frac{F_m}{F_m^o} = k\frac{F_m}{\text{PCSA}}, \tag{15}$$

where F_m/PCSA is muscle stress, PCSA is physiological cross-sectional area, and k is a constant. In the physiological case (Eq. (12)), muscle activation is approximately equal to muscle stress multiplied by some proportionality constant, provided a muscle operates on the flat portion of its force-length curve and at small contraction velocities:

$$a_m = \frac{F_m}{f(F_m^o, l_m, v_m)} \approx k\frac{F_m}{PCSA} \quad \text{when } l_m \approx l_m^o \quad \text{and}$$
$$v_m \approx 0.0. \tag{16}$$

where l_m^o is the optimal muscle-fiber length.

Thus, the non-physiological static optimization problem was to find an activation level for each muscle in the model such that the performance criterion (Eq. (14)) was minimized, the joint torques predicted by the dynamic optimization solution (Eq. (13)) were generated at each joint, and each muscle was treated as an ideal force generator (Eq. (11)). The physiological static optimization problem was the same, except that each muscle was constrained to act in accordance with its force–length–velocity properties (Eq. (12)). Both static optimization problems were solved using a gradient-based sequential quadratic programming algorithm (Pandy et al., 1992).

3. Results

The joint moments predicted by the dynamic optimization solution (and used as input to the static optimization problem) were similar to those reported in the literature (Figs. 3 and 4) (Cappozzo et al., 1975; Crowninshield et al., 1978; Patriarco et al., 1981; Inman et al., 1981). Joint moments about the axes of the back, subtalar, and metatarsal joints were also predicted by the dynamic solution but are not reported here. Discontinuities in the joint torques are present because the terminal boundary constraints imposed in the dynamic optimization solution were not precisely met.

In general, the forces predicted by the dynamic and static solutions were very similar for many muscles (Figs 5 and 6: ILPSO, GMAXL, GMEDA, VAS, GAS, SOL, TFL, BFSH, PFEV). However, there were two notable exceptions. Following heelstrike, the dynamic solution predicted significant activity in the medial portion of gluteus maximus, whereas the static solutions predicted very little activity in this muscle (Fig. 5: GMAXM, 0–30%). On the other hand, the static solutions predicted significant activity in hamstrings, whereas the dynamic solution predicted much less activity in this muscle (Fig. 5: HAMS, 0–30%).

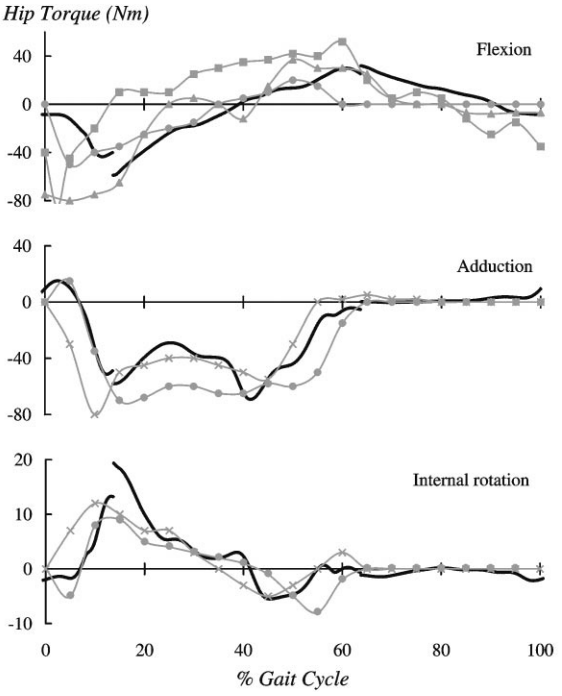

Fig. 3. The net muscle moments applied about the axes of the hip joint are shown as predicted by the dynamic optimization solution (thick black lines) and as measured by Crowninshield et al. (1978) (circles), Cappozzo et al. (1975) (triangles), Patriarco et al. (1981) (crosses), and Inman et al. (1981) (squares).

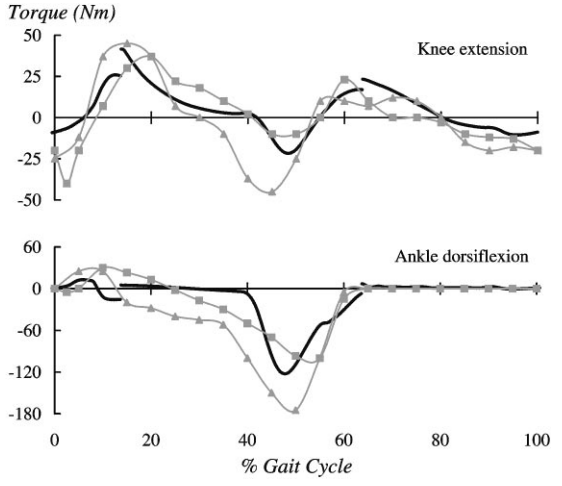

Fig. 4. The net muscle moments applied about the axes of the knee and ankle joints are shown as predicted by the dynamic optimization solution (thick black lines) and as measured by Cappozzo et al. (1975) (triangles) and Inman et al. (1981) (squares).

The resultant joint contact forces at the hip, knee, and ankle predicted by the dynamic and both static optimization solutions were very similar to each other and somewhat similar to contact forces reported by Crowninshield and Brand (1981) and Hardt (1978) (Fig. 7). For both the

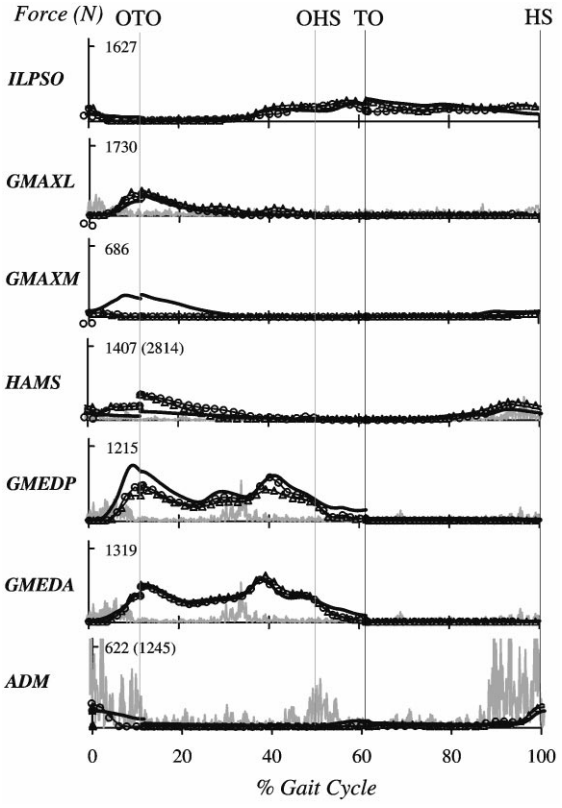

Fig. 5. Forces generated by muscles spanning the hip and knee. The muscle forces predicted by the dynamic solution (thick black lines), by the physiological static solution (circles), and by the non-physiological static solution (triangles) are shown as a percentage of the gait cycle. See Fig. 1 for the muscle abbreviations. EMG data from one subject are shown in thin grey lines. The following gait cycle landmarks are demarcated by thin vertical lines: opposite toe-off (OTO), opposite heel-strike (OHS), toe-off (TO), and heel-strike (HS). The plots are scaled to each muscle's maximum isometric strength. In several cases, where a number is shown in parentheses, the plot is scaled to half the muscle's maximum isometric strength to provide a more effective scale for viewing the data. In general, the forces predicted by the different solutions were similar. However, following HS (0–30%), the force generated by GMAXM was much larger in the dynamic solution than in the static solutions. The reverse was true for HAMS during the same time period. Also note that just prior to TO (55–62%), the forces in GMEDP and GMEDA fell more gradually in the dynamic solution than in the static solutions.

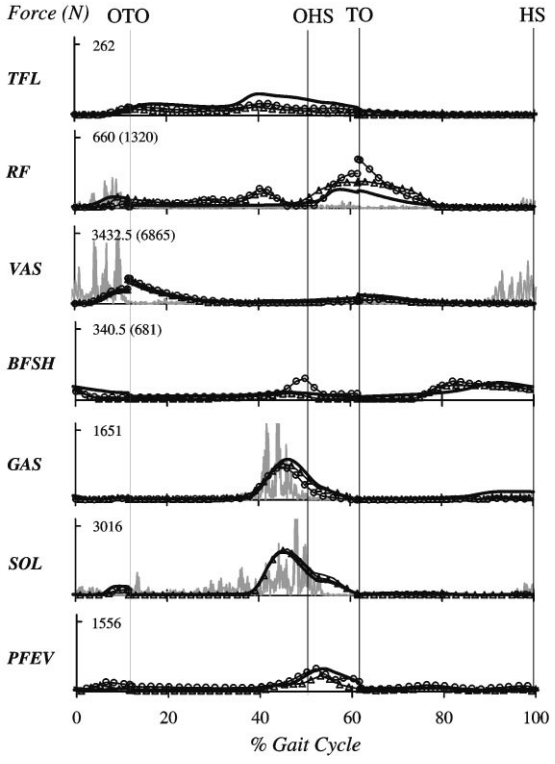

Fig. 6. Forces generated by muscles spanning the hip, knee, and ankle. The muscle forces predicted by the dynamic solution (thick black lines), by the physiological static solution (circles), and by the non-physiological static solution (triangles) are shown as a percentage of the gait cycle. See Fig. 1 for the muscle abbreviations. EMG data from one subject are shown in thin grey lines. The following gait cycle landmarks are demarcated by thin vertical lines: opposite toe-off (OTO), opposite heel-strike (OHS), toe-off (TO), and heel-strike (HS). The plots are scaled to each muscle's maximum isometric strength. In several cases, where a number is shown in parentheses, the plot is scaled to half the muscle's maximum isometric strength to provide a more effective scale for viewing the data. In general, the forces predicted by the different solutions were similar.

static and dynamic solutions, peak contact forces were about 4.0 times body weight at the hip, about 2.7 times body weight at the knee, and nearly 6.0 times body weight at the ankle. Contact forces at the ankle were large compared to those computed by Hardt (1978), perhaps because the moment arms of the plantarflexors were underestimated or because excessive torque about the subtalar axis was demanded in our model. Following heel-strike, the static optimization solutions did predict a contact force at the knee which was about one-half body weight greater than that predicted by the dynamic solution (Fig. 7, Knee, 0–30%). Also, during push-off, the dynamic solution predicted a contact force at the hip which fell more slowly than the hip contact forces predicted by the static solutions (Fig. 7, Hip, 55–62%).

4. Discussion

The design of the current study allows a comparison of static and dynamic optimization in the absence of experimental error. In addition, the complexity of the musculoskeletal model used in this study allows an evaluation of the static optimization approach as it has been used since the early 1980s to estimate muscle forces during gait. Conservatively, the dynamic solution required 1000 times more computation time than either of the static solutions. However, the similarity of the static solutions and the dynamic solution suggests that this computational expenditure does not significantly

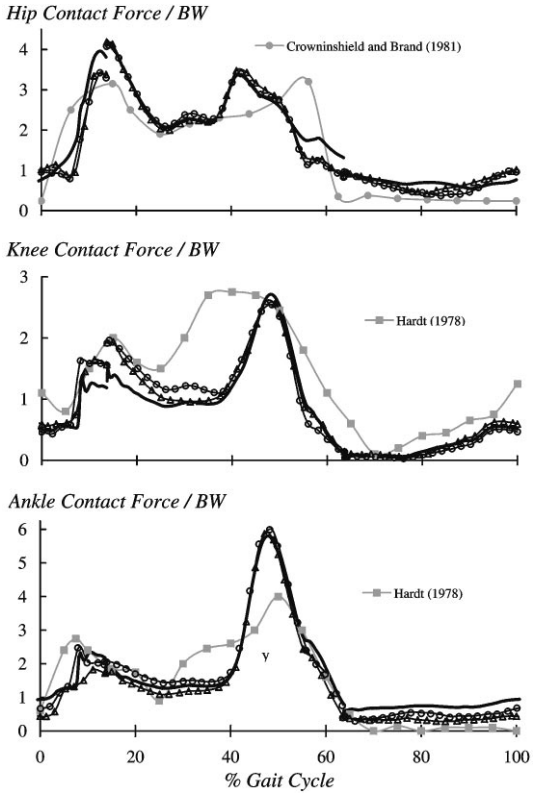

Fig. 7. Joint contact force in the hip, knee, and ankle. The resultant joint contact forces normalized by body weight are shown as a percentage of the gait cycle, as predicted by the dynamic solution (thick black lines), the physiological static solution (circles), and the non-physiological static solution (triangles). Also shown are contact forces published by Crowninshield and Brand (1981) (filled grey circles) and Hardt (1978) (filled grey squares). The predicted contact forces were very similar except at the knee following heel-strike (10–30%) and at the hip prior to toe-off (55–62%).

improve predictions of muscle or joint contact forces. Regarding static optimization problems for normal gait, it appears that a time-independent performance criterion is adequate and, further, that both activation dynamics and the force–length–velocity properties of muscle can be neglected.

The static performance criterion used in this study was essentially the same as the squared muscle-stress criterion used by Crowninshield and Brand (1981) (Eqs. (14)–(16))[1]. They argued that minimizing muscle stress raised to a power between 1.4 and 5.1 is physiologically analogous to minimizing muscle fatigue.[2] We tried powers of 2, 3, and 4, and chose a power of 2 because this choice resulted in the greatest similarity between our static and dynamic solutions. The striking similarity between the muscle forces predicted by the static solutions and the dynamic solution (Figs. 5 and 6) suggests that minimizing muscle fatigue at each instant is roughly the same as minimizing metabolic energy expended per unit distance traveled over the duration of the gait cycle (Eq. (9)). Thus, the use of a time-independent performance criterion does not appear to be a significant limitation when solving static optimization problems for gait.

We believe the difference in knee contact force shown in Fig. 7 was driven by differences between the static and dynamic performance criteria. In the dynamic solution, GMAXM developed substantial force, whereas in the static solutions HAMS was activated in preference to GMAXM (Fig. 5, 0–30%). Since HAMS is a biarticular muscle, it contributes to contact force at the knee as well as the hip. It is difficult to say which solution is more realistic; the extent to which HAMS is used during gait might vary greatly across individuals. Perhaps it is best to interpret the differences between the static and dynamic solutions as suggesting a range of contact forces which might be present in the knee during gait, depending on one's coordination strategy.

The similarity between the force trajectories for the physiological and non-physiological static solutions reveals that the force–length–velocity properties of muscle had surprisingly little impact on the static solutions. This is likely due to the fact that the force demanded from each muscle in the model was well within the limits defined by its force–length–velocity surface.

The similarity between the static and dynamic solutions also suggests that activation dynamics does not need to be explicitly accounted for when solving static optimization problems for normal gait. Since the joint torques used to drive the static problems were generated by integrating Eq. (2), among other state equations, they were consistent with the rise and fall time constants for muscle activation. Therefore, it is not surprising that the static solutions were also *roughly* consistent with activation dynamics.

Both static solutions appear to have been inconsistent with activation dynamics in one notable instance: the smaller hip contact forces developed prior to toe-off during the static solutions fell too rapidly (Fig. 7, Hip,

[1] We re-solved the static problems minimizing the square of muscle stress instead of activation, and there was almost no change in the predicted muscle *forces*. The benefit of expressing the performance criterion in terms of activation was that the predicted muscle *activations* agreed much better with recorded EMG for muscles which approached the extremes of their force length curves (e.g., GAS during push-off) (*unpublished results*).

[2] Dul et al. (1984) also formulated a minimum fatigue criterion which accounts for muscle fiber type, and this criterion has been shown to provide better in vivo estimates of muscle force in walking cats (Herzog and Leonard, 1991; Prilutsky et al., 1997). Unfortunately, using the Dul et al. (1984) criterion to solve static optimization problems for systems with many degrees of freedom and many muscles is computationally challenging. We are therefore unable to comment on which fatigue criterion might be best for human gait.

55–62%). Most of the force difference at the hip originated from GMEDP and GMEDA (Fig. 5). The activation levels of these muscles were falling prior to toe-off. In the dynamic optimization solution, the fall was governed by the differential equation for activation dynamics (Eq. (2)), while in the static optimization solutions the muscle activation levels fell at non-physiological rates. In this case, the dynamic solution arguably provided the more accurate estimates of muscle and joint contact force.

The current analysis is limited in at least two respects. First, the results pertain to normal gait and may not extend to other activities. Second, the similarity between the dynamic and static optimization solutions could have been influenced by the number of muscles in the model. On average, there are just over three muscles for each joint axis in the model. If the number of muscles were increased and the control of the system thus made more redundant, it is possible that differences in the predicted muscle forces between the dynamic optimization solution and static optimization solutions would become more pronounced. However, while greater differences might emerge in the predicted muscle forces, we believe that these differences would have little impact on the predicted resultant joint contact forces. For the most part, increasing the number of muscles in the model would mean simply separating combined muscles in our model into individual muscles (e.g., HAMS into biceps femoris long head, semitendionosis, and semimembranosus). Because the new muscles would have approximately the same moment arms as the combined muscle they replaced, the predicted resultant joint contact forces would be roughly the same.

To conclude, if one can accurately solve the inverse dynamics problem for normal gait, and if one seeks only to estimate muscle and joint contact forces, the use of dynamic optimization in preference to static optimization is currently not justified. Further, when solving static optimization problems for normal gait, both the force–length–velocity properties of muscle and activation dynamics can be neglected without resulting in significant changes in the predicted muscle and joint contact forces.

While the findings of this paper support the use of static optimization to estimate contact forces during normal gait, they do not imply that dynamic optimization should not be used at all. Dynamic optimization may be preferred or even necessary when:

1. *Accurate experimental data are not available.* Dynamic optimization often requires only a set of initial states and is not strongly dependent on the accuracy of the input kinematic data.

2. *Activation dynamics plays an important role.* For certain activities (e.g., sprint cycling (Martin et al., 2000)), it might be necessary for activation dynamics to be explicitly incorporated in the solution process. Dynamic optimization provides a natural framework for doing so.

3. *An appropriate time-independent performance criterion is not available.* Some activities may be characterized inherently by a time-dependent performance criterion (e.g., maximum-height jumping; Pandy et al., 1990). Such criteria can be evaluated only by using a forward dynamics approach.

4. *The ability to predict novel movement is desired.* A forward dynamics approach need not only address the force distribution problem. When combined with some sort of high-level goal setting (e.g., a performance criterion), it is capable of predicting novel movement. Because of this, dynamic optimization offers a powerful framework for investigating the influences of musculoskeletal structure on biomechanical performance. In contrast, static optimization is what we would term a "descriptive" methodology in which the motion undertaken by the model is prescribed by the measured kinematics.

We believe that static and dynamic optimization should be viewed as complementary approaches. Static optimization provides a practical and computationally inexpensive method of descriptively estimating in vivo quantities like muscle and joint contact forces. When estimates of these quantities are insufficient for understanding movement, dynamic optimization offers a more powerful, although more costly, alternative.

Acknowledgements

Partial funding for this work was provided by the Whitaker Foundation and by NASA, Grant No NAG5-2217. We also gratefully acknowledge support of the NASA/Ames Research Center and the Center for High Performance Computing at The University of Texas at Austin.

References

An, K.N., Kaufman, K.R., Chao, E.Y.S., 1989. Physiological considerations of muscle force through the elbow joint. Journal of Biomechanics 22, 1249–1256.

Anderson, F.C., 1999. A dynamic optimization solution for a complete cycle of normal gait. Ph.D. Thesis, The University of Texas at Austin, Austin, Texas.

Anderson, F.C., Pandy, M.G., 1999. A dynamic optimization solution for vertical jumping in three dimensions. Computer Methods in Biomechanics and Biomedical Engineering 2, 201–231.

Anderson, F.C., Pandy, M.G. Dynamic optimization of human walking. Journal of Biomechanical Engineering, submitted for publication.

Anderson, F.C., Ziegler, J.M., Pandy, M.G., Whalen, R.T., 1995. Application of high-performance computing to numerical simulation of human movement. Journal of Biomechanical Engineering 117, 155–157.

Brand, R.A., Pedersen, D.R., Friederich, J.A., 1986. The sensitivity of muscle force predictions to changes in physiologic cross-sectional area. Journal of Biomechanics 19, 589–596.

Cappozzo, A., Leo, T., Pedotti, A., 1975. A general computing method for the analysis of human locomotion. Journal of Biomechanics 8, 307–320.

Chow, C.K., Jacobson, D.H., 1971. Studies of human locomotion via optimal programming. Mathematical Biosciences 10, 239–306.

Corcoran, P.J., Brengelmann, G.L., 1970. Oxygen uptake in normal and handicapped subjects, in relation to speed of walking beside velocity-controlled cart. Archives of Physical Medicine and Rehabilitation 51, 78–87.

Crowninshield, R.D., Brand, R.A., 1981. A physiologically based criterion of muscle force prediction in locomotion. Journal of Biomechanics 14, 793–801.

Crowninshield, R.D., Johnston, R.C., Andrews, J.G., Brand, R.A., 1978. A biomechanical investigation of the human hip. Journal of Biomechanics 11, 75–85.

Davy, D.T., Audu, M.L., 1987. A dynamic optimization technique for predicting muscle forces in the swing phase of gait. Journal of Biomechanics 20, 187–201.

Delp, S.L., 1990. Surgery simulation: a computer graphics system to analyze and design musculoskeletal reconstructions of the lower limb. Ph.D. Thesis, Stanford University, Stanford, California.

Dul, J., Johnson, G.E., Shiavi, R., Townsend, M.A., 1984. Muscle synergism-II. A minimum-fatigue criterion for load sharing between synergistic muscles. Journal of Biomechanics 17, 675–684.

Finley, F.R., Cody, K.A., 1970. Locomotive characteristics of urban pedestrians. Archives of Physical Medicine and Rehabilitation 51, 423.

Glitsch, U., Baumann, W., 1997. The three-dimensional determination of internal loads in the lower extremity. Journal of Biomechanics 30, 1123–1131.

Hardt, D.E., 1978. Determining muscle forces in the leg during human walking: an application and evaluation of optimization methods. Journal of Biomechancal Engineering 100, 72–78.

Hatze, H., 1976. The complete optimization of human motion. Mathematical Biosciences 28, 99–135.

Hatze, H., Buys, J.D., 1977. Energy-optimal controls in the mammalian neuromuscular system. Biological Cybernetics 27, 9–20.

Herzog, W., Leonard, T.R., 1991. Validation of optimization models that estimate the forces exerted by synergistic muscles. Journal of Biomechanics 24 (Suppl. 1), 31–39.

Inman, V.T., 1976. The Joints of the Ankle. The Williams & Wilkins Company, Baltimore.

Inman, V.T., Ralston, H.J., Tood, F., 1981. Human Walking. Williams and Wilkins, Baltimore.

Kaufman, K.R., An, K.N., Litchy, W.J., Chao, E.Y.S., 1991. Physiological prediction of muscle forces- II. Application to isokinetic exercise. Neuroscience 40, 793–804.

Kautz, S.A., Neptune, R.R., Zajac, F.E., 2000. General coordination principles elucidated by forward dynamics: Minimum fatigue does not explain muscle excitation in dynamic tasks. Motor Control 4, 75–80.

Martin, J.C., Brown, N.A., Anderson, F.C., Spirduso, W.W., 2000. A governing relationship for repetitive muscular contraction. Journal of Biomechanics 33, 969–974.

McConville, J.T., Clauser, C.E., Churchill, T.D., Cuzzi, J., Kaleps, I., 1980. Anthropometric relationships of body and body segment moments of inertia. Technical Report AFAMRL-TR-80-119. Air Force Aerospace medical Research Laboratory, Wright-Patterson AFB, Ohio.

Mommaerts, W.F.H.M., 1969. Energetics of muscular contraction. Physiological Reviews 49, 427–508.

Pandy, M.G., Garner, B.A., Anderson, F.C., 1995. Optimal control of non-ballistic muscular movements: A constraint-based performance criterion for rising from a chair. Journal of Biomechanical Engineering 117, 15–26.

Pandy, M.G., Anderson, F.C., Hull, D.G., 1992. A parameter optimization approach for the optimal control of large-scale musculoskeletal systems. Journal of Biomechanical Engineering 114, 450–460.

Pandy, M.G., Zajac, F.E., Sim, E., Levine, W.S., 1990. An optimal control model for maximum-height human jumping. Journal of Biomechanics 23, 1185–1198.

Patriarco, A.G., Mann, R.W., Simon, S.R., Mansour, J.M., 1981. An evaluation of the approaches of optimization models in the prediction of muscle forces during human gait. Journal of Biomechanics 14, 513–525.

Pedersen, D.R., Brand, R.A., Davy, D.T., 1997. Pelvic muscle and acetabular contact forces during gait. Journal of Biomechanics 30, 959–965.

Pedotti, A., Krishnan, V.V., Stark, L., 1978. Optimization of muscle-force sequencing in human locomotion. Mathematical Biosciences 38, 57–76.

Prilutsky, B.I., Herzog, W., Allinger, T.L., 1997. Forces of individual cat ankle extensor muscles during locomotion predicted using static optimization. Journal of Biomechanics 30, 1025–1033.

Ralston, H.J., 1958. Energy-speed relation to optimal speed during level walking. Internationale Zertschrift Angewandte fuer Physiologie 17, 277–283.

Ralston, H.J., 1976. Energetics of human walking. In: Herman, R.M., Grillner, S., Stein, P.S.G., Stuart, D.G. (Eds.), Neural Control of Locomotion. Plenum Press, New York, pp. 77–98.

Röhrle, H., Scholten, R., Sigolotto, C., Sollbach, W., 1984. Joint forces in the human pelvis-leg skeleton during walking. Journal of Biomechanics 17, 409–424.

Seireg, A., Arvikar, R.J., 1975. The prediction of muscular load sharing and joint forces in the lower extremities during walking. Journal of Biomechanics 8, 89–102.

Tashman, S., Zajac, F.E., Perkash, I., 1995. Modeling and simulation of paraplegic ambulation in a reciprocating gait orthoses. Journal of Biomechanical Engineering 117, 300–308.

Yamaguchi, G.T., Zajac, F.E., 1990. Restoring unassisted natural gait to paraplegics via functional neuromuscular stimulation: a computer simulation study. IEEE Transactions on Biomedical Engineering 37, 886–902.

Zajac, F.E., 1989. Muscle and tendon: properties, models, scaling, and application to biomechanics and motor control. In: Bourne, J.R. (Ed.), CRC Critical Reviews in Biomedical Engineering., Vol. 19. CRC Press, Boca Raton, pp. 359–411.

Zajac, F.E., 1993. Muscle coordination of movement: a perspective. Journal of Biomechanics 26 (Suppl. 1), 109–124.